MODELING AND SIMULATION OF ION IMPLANTATION AND ELECTRICAL DISCHARGE DEPOSITION

Iuga Ana Cristina [1], Liviu Daniel Ghiculescu[2]
[1] Polytechnic University of Bucharest, Faculty of Industrial Engineering and Robotics, iugaanacristina@gmail.com
[2] Polytechnic University of Bucharest, Faculty of Industrial Engineering and Robotics, daniel.ghiculescu@gmail.com

ABSTRACT: This paper deals with the modelling and simulation of an ion implantation installation and deposition of microstructures on an Aluminum 7075 plate. COMSOL Multiphysics was used to study the ion implantation process on surface of the sample. Within an ion implanter, ions generated within thermo emissive cathode are accelerated by an electric field to achieve the desired implant energy. The energy dose and angle of the ion incident beam are both key parameters for the process. By changing the placement angle of the plate incrementally by five degrees, the number density, the variation of the molecular flux and the pressure were simulated. It was approached another related process involving ion deposition – electrical discharge deposition (EDD) – based on modeling and simulation of the process through mentioned above dedicated software. The process parameters were determined aiming at material deposition on the sample and keeping under control the deposition dimensions.
KEYWORDS: ion implantation, electrical discharge deposition, modeling, simulation.

1. INTRODUCTION

Aluminum and its alloys are used on a large scale in the aerospace, automotive, marine, chemical, and electronics industries due to their low density, relative low price, high wear resistance, and great strength [1]. But the application of aluminum alloys is constrained by its relatively high chemical reactivity with working environment factors and poor corrosion resistance. An oxide layer could be formed and thus the corrosion resistance could brow, this layer being effortlessly eroded. This phenomenon could be the result of the defects within the oxide layers, and more probability of exposure to the atmospheric agents and attack from chloride ions, more corrosion cracks occurring [1,2]. Given the fact that it is a material that has high strength in stressed structural parts, AA7075 is an aluminum alloy that it is used in different applications: airspace, shafts, gears, aircraft, and defense applications.

On the surface of this aluminum alloy the quality can be improved by different surface coatings. The techniques that can be applied are: Physical Vapor Deposition (PVD), Chemical Vapor Deposition (CVD) or Ion Implantation (II), and even Electrical Discharge Deposition (EDD). Some researchers have shown that tribology properties as hardness, wear resistance, fatigue life and corrosion of the AA7075 could be increased using nitrogen ion beam implantation [3,4].

Ion implantation is the technological process by which the ion beam is accelerated, directed an implanted within a solid material [5].

This study approached the design of an ion implantation system using the Molecular Flow module from COMSOL Multiphysics. The average density of the number of molecules along the beam path is used as a merit value to evaluate the design, because the interactions between the molecules that released with the beam produce unwanted species. Since there is an axis of rotation, the angle of the wafer (sample) to the beam can be changed, and the merit figure depends on to this angle [6].

The effects of this ion implantation could be observed by investigating the changes in the microstructure of aluminum alloy AA7075 and on its the mechanical properties.

The EDD process is somehow similar to ion implantation, but ion beams are generated by electrical discharges in a gas, forming a plasma channel, and the electric loads can be directed by an aiding magnetic field. Considering the process performed on a classic EDM installation with additional magnetic facilities, lower cost than the first variant in vacuum setting could be obtained.

2. STAGES OF ION IMPLANTATION

The stages of ion implantation are:

- At a pressure of less that 10^{-2} Pa the system is vacuumed;
- At a voltage of 2…5 kV and a cathodic current density of 0.3...0.6 mA/cm^2 the argon is introduced up to pressure of 1…5 Pa to produce ionization by preparing the gas discharge;
- At the evaporation temperature of the material, the deposition begins by gradually raising the temperature of the vapor source. The shutter between the source-material and the substrate is removed to allow the deposition on the substrate;
- A balance is established among the spray and

deposition rate for the surface layer composition;
• This process continues until the desired thickness of the superficial layer is reached.
In the ion implantation process, there are certain parameters that must be controlled to obtain a reproducible deposit with needed properties: waste gas pressure, inert gas pressure, deposit rate, source-substrate distance, the substrate electronic potential, ionic current density, spray cleaning duration.
Depending on the energy of the accelerated ions, the penetration depth can be determined experimentally or calculated with the formula [7]:

$$R_{max} = \alpha_R \cdot \sqrt{E} \quad [\mu m] \qquad (1)$$

where: R_{max} represents the maximum penetration depth of the particles [μm]; α_R - a constant that depends on the ion nature and physic-chemical state of the source, and E - the energy of the ions [keV].
Ion trajectory and path distribution (path deviation) is of utmost interest in ion implantation process. The distribution of ions in different transversal planes of their path is approached by numerical simulation.

3. PAREMETERS OF ELECTRICAL DISCHARGES DEPOSITION

To create a hard layer on the surface of AA7075, Electro Discharge Deposition (EDD) can be used. This technology - the reverse process of EDM - modifies the surface of the sample, extending with an anti-wear coating. The condition for using EDD is electrically conductive material, the case of Al alloys. A higher percentage of the supplied energy is allocated to the anode, approximate 45% at the anode, and only 25% at the cathode. For the fastest wear of the tool, i.e. its material deposition on the workpiece, the reverse polarity is used, that is the tool must be connected to the positive terminal [8]. The dielectric used is nitrogen (an inert gas) because would aid in better deposition process [9]. Compared to dielectric liquid that have a breakdown voltage of 10kV/mm, the gases have less than 3kV/mm and are insulators too. For preventing the changes of arcing during the process, the gases recover immediately after discharge, so that the next discharge occurs immediately. The uniformity of the deposit layer increase being useful in generating ultra-small discharges [10]. At EDM, the negative polarity is useful in this case, but EDD being its reverse process, the positive one (tool anode) is suitable.
This EDD process was performed using an EDM machine and varying the factors: current, pulse on time, duty factor (ratio between on and off time) and voltage. Studies have shown that the magnetic field can be used (process hybridization) to improve the quality of the deposition, i.e. controlling the deposit dimensions: the height, weight and width [11].
Table 1 shows some values of the parameters that can be modified to perform the deposition process. Since the process is hybrid, it contains EDM parameters (1-4) and magnetic flux (5).

Table 1. The mechanism of magnetic field deposition process [11]

No.	Parameters	Levels				
1.	Current (I), A	3	9	14	19	25
2.	Pulse on time (T_{on}), μs	7.5	20	30	40	50
3.	Duty factor (t)	2	5	7	9	12
4.	Voltage (v), V	2	30	50	70	98
5.	Magnetic flux, Tesla	0.04	0.07	0.16	0.20	0.40

4. IMPROVEMENTS OF SURFACE LAYER BY NITROGEN IMPLANTATION

4.1. Hardness measurements

The hardness increases due to the collision between nitrogen ions with the material during the process of ion implantation in aluminum alloys, causing the detachment of atoms from its orbit.
The new AlN layer is formed when nitrogen ions fill that void. After reaching the optimum dose, the hardness will decrease to 27.3 VHN, because the collision gap is already full. The hardness will decrease as more ions are added, causing defects on the surface of the material [12].

4.2. Corrosion Test

Some electrochemical measurements were effectuated by three Potensio Galvanostat VersStat 4 electrodes in 3.5% NaCl solution. Thus, the implanted samples of 1 cm^2, were exposed to the corrosion environment.

Potential dynamics currents were determined in the interval -250 mV cathodic and 250 mV anodic of sample polarization with respect to the potential of the open circuit at a scan rate of 5 mVs^{-1}. Tafel graphs calculate potential dynamic polarization parameters such as corrosion potential (Ecorr), corrosion current (icorr), polarization resistance (Rp), anodic and cathodic slopes (ba and bc) and corrosion rate.

There is a change of the Ecorr corrosion potential from - 0, 410,378 mV to - 399,951 mV and there is a reduction of the corrosion rate from 0.012 mmpy to 0.011 mmpy [13].

4.3. Roughness Measurement

On the implanted surface, the average roughness value (Ra) is 37.5 nm and the average root square (RMS) is 47.6 nm. On analysis under a microscope there are cone-shaped hills. Their distribution was almost uniform, caused by the penetration of the high energy nitrogen ion into the AA7075 aluminum alloy. So, the ionic implantation changes the structure of the surface, hence the roughness [14].

5. MODELING AND SIMULATION

The vacuum system was designed using the Autodesk Inventor Professional 2021 program and imported into the COMSOL Multiphysics 5.5 program. The model geometry is shown in Figure 1.

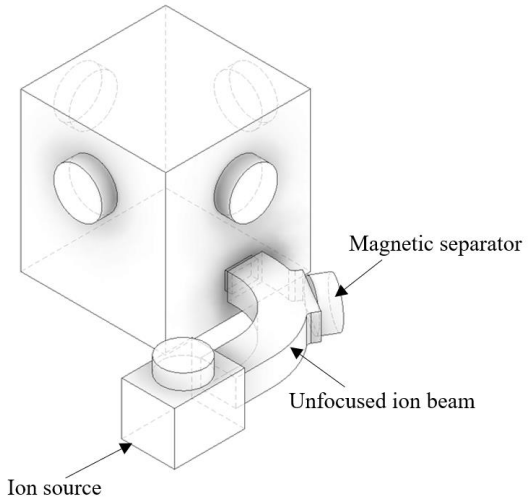

Figure 1. Vacuum system

COMSOL Multiphysics was used starting with space dimension, the physics module and the type of the study as follows: 3D – Rarefied Flow – Free Molecular Flow – Stationary.

The sample of AA 7075 is positioned on a carrier plate which is rotated around an axis (red line, Figure 2) through its center to obtain different implant angles. The carrier plate is mounted in a chamber that is supplied by five cryopumps, on cylindrical vacuum ports, with certain pump speed (pcs). The total gas emitted across the wafer surface is uniform as outgassing. [6].

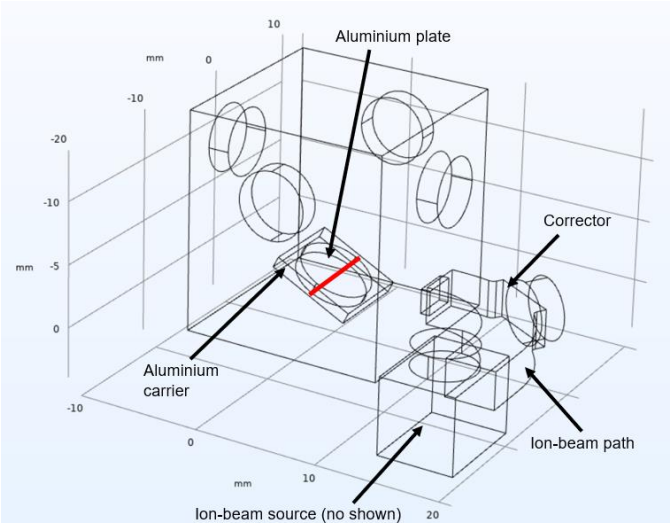

Figure 2. Ion implantation system

The vacuum path enters through the magnetic separator placed opposite the wafer and is pumped by a turbo-molecular pump, next to corrector on a cylindrical port, with a certain speed, *ps* and a cryopump at the start of the beam path, with a pump speed, *pcs*. The angle of the aluminum plate normal to the ion beam is swept from 30º to 60º in 5º steps, as the aluminum plate is rotated about the horizontal axis through its center, as shown in Figure 2. This system has in its structure a flow pump, Figure 3, and also five cryogenic pumps, Figure 4, that provide that vacuum and liquefy the particles emitted by nitrogen.

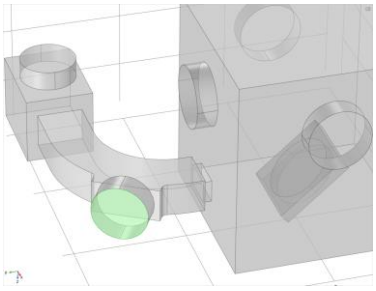

Figure 3. Flow pump selection

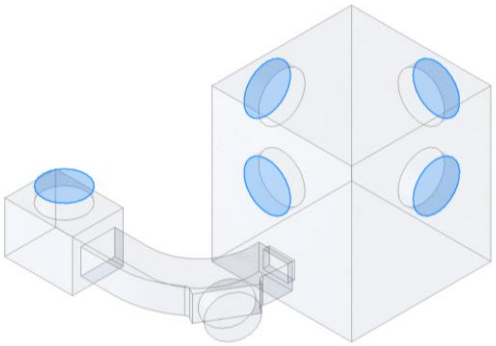

Figure 4. Cryogenic pumps

Parameters

Name	Expression	Value	Description
theta	30	30	Wafer angle
pumpspeedcryo	12000[l/s]	12 m^3/s	Pump speed for cryo
pumpspeedturbo	1500[l/s]	1.5 m^3/s	Pump speed for turbo

Figure 5. Parameters

The main parameters used for ion implantation modeling are shown in Figure 5. These allow to change the flow for the cryopump, turbo pump as well as the wafer (plate) angle.

In order to create de geometry of the wafer, it was necessary to introduce a plane of the coordinate type, containing the wafer surface to be implanted, its modeling and the extrusion of the geometry being represented in Figure 6.

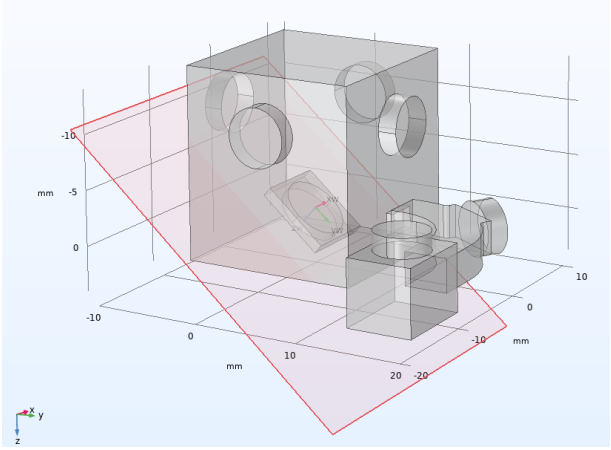

Figure 6. Modeling of the plane with the implant surface

The next step was to allocate materials from COMSOL's library. AA 7075 is assigned to the extruded plate (Figure 7) and nitrogen fills the whole vacuum system (Figure 8).

Material Contents

Property	Variable	Value	Unit	Property group
Thermal conductivity	k_iso ; kii...	k_solid_T6_as...	W/(m·K)	Basic
Coefficient of thermal expansion	alpha_iso ;...	(alpha(T[1/K])...	1/K	Basic
Heat capacity at constant pressure	Cp	C(T[1/K])[J/(...	J/(kg·K)	Basic

Figure 7. Aliminium's properties (AA 7075)

Material Contents

Property	Variable	Value	Unit	Property group
Dynamic viscosity	mu	eta(T)	Pa·s	Basic
Ratio of specific heats	gamma	1.4	1	Basic
Heat capacity at constant pressure	Cp	Cp(T)	J/(kg·K)	Basic

Figure 8. Nitrogen's properties

Nitrogen is released from the highlighted surface that is shown in Figure 9.

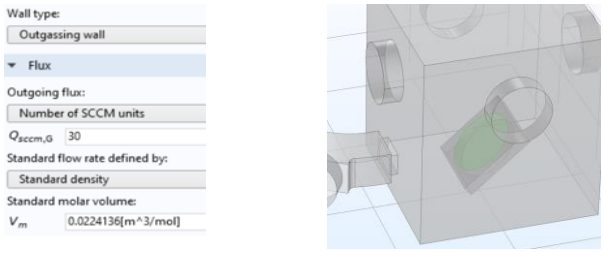

Figure 9. Presentation of the property of the highlighted surface

In Figure 11 it's presented a statistic of the meshing network.

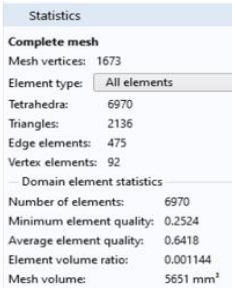

Figure 10. Mesh selection

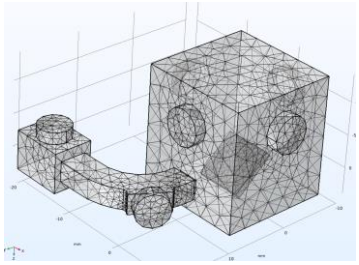

Figure 11. Meshing statistics

By running the program, the purpose was to highlight the effects that occur on the surface of the sample in terms of molecular flux, Figure 12, numerical density, Figure 13 and total pressure, Figure 14.

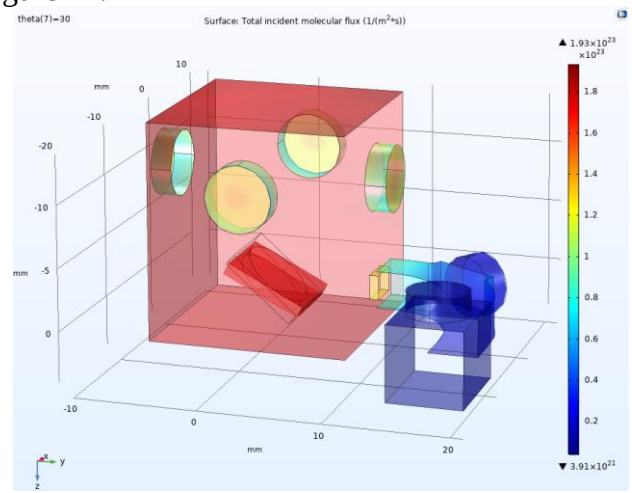

Figure 12. Total incident molecular flux

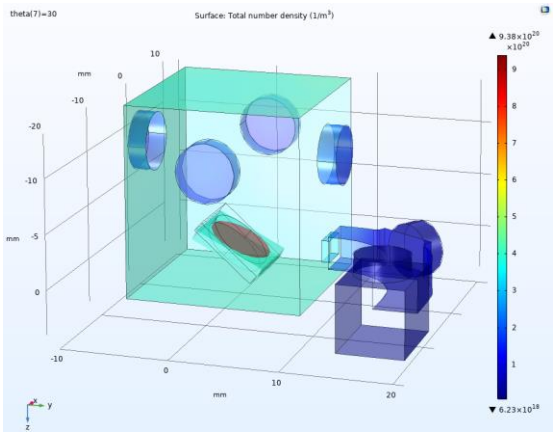

Figure 13. Total number density

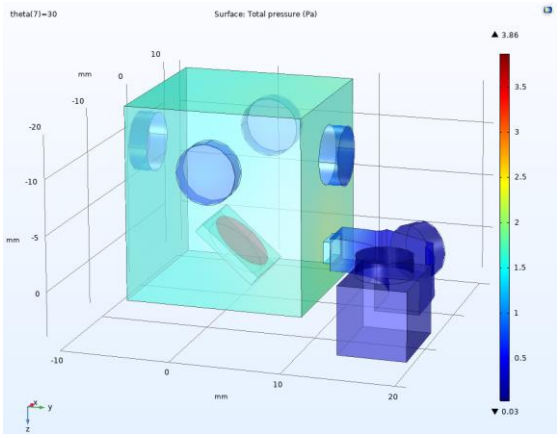

Figure 14. Total pressure

5.1. Modeling and simulation of the magnetic field at EDD

For the related technology, EDD, the modeling and simulation of the ion trajectory in the magnetic field was performed using Comsol Multiphysics 5.5, successively accessing: 3D – AC/DC – Magnetic Fields – Stationary, in stage 1, coupled with Charged Particle Tracing module, in stage 2.

The parameters shown in Figure 15 were used to design: the anode, coil and working space (equivalent of collimator), and at target distance, bottom of the working space was placed the sample - Figure 16.

Parameters

Name	Expression	Value	Description
Ic	0.4[A]	0.4 A	current in the coil
Nc	3000	3000	number of turns
rbe	3	3	outer radius coil
hb	0.75	0.75	coil height
rbi	1.75	1.75	inner radius coil
rcol	7.5	7.5	workspace radius
hcol	9	9	column height
scol	3	3	target distance in the column
hc	4	4	anode height
rc	0.1	0.1	anode radius
dc	1	1	distant anode_coil
E0	500[eV]	8.0109E-17 J	initial energy
V0	(2*E0/me_const)^0.5	1.3262E7 m/s	initial speed of electrons
tpar	0.001*scol/V0	2.2621E-10 s/m	target distance travel time
tp	5e-9	5E-9	study time
Jsz	550000	5.5E5	surface current density
Np	1000	1000	number of particles
mazot	14*1.66053906660e-27	2.3248E-26	nitrogen ion mass
Vazot	sqrt(2*8.01e-17/mazot)	83012	nitrogen ion velocity
tpN	scol/Vazot	3.6139E-5	nitrogen ion travel time
tps	10e-4	0.001	nitrogen ion study time

Figure 15. Parameters added in Global definitions

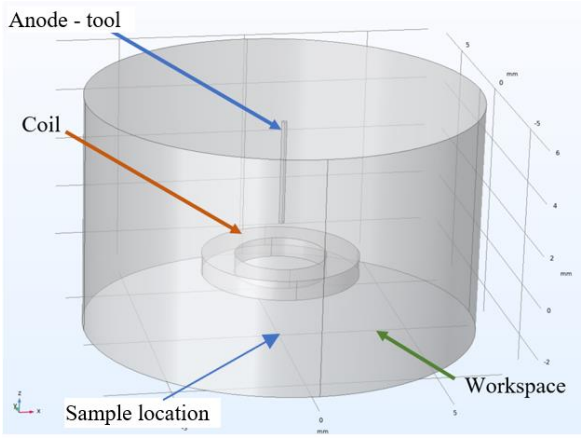

Figure 16. Geometry of the model

The materials were allocated to the model: air was assigned to the workspace (Figure 17), and copper for the coil and the anode tool (Figure 18).

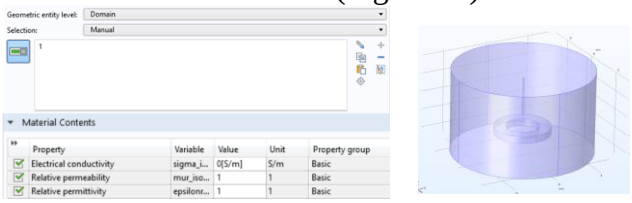

Figure 17. Material allocation for the collimator

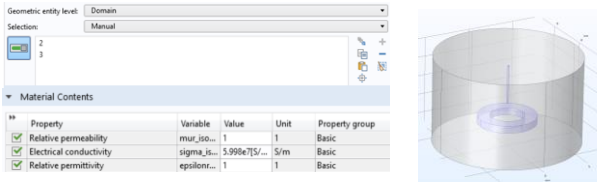

Figure 18. Material allocation for the cathode and coil

Discretization is done with precise, tetrahedral elements (choosing the finer grade) and its Statistics is presented in Figure 19.

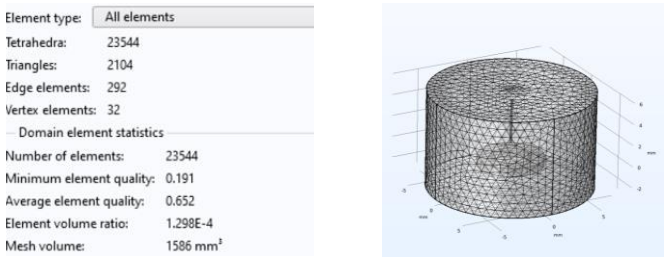

Figure 19. Mesh selection and quality

Surface Current Density is added as a parameter that determined the magnetic force exerted on the ion beam (Figure 20).

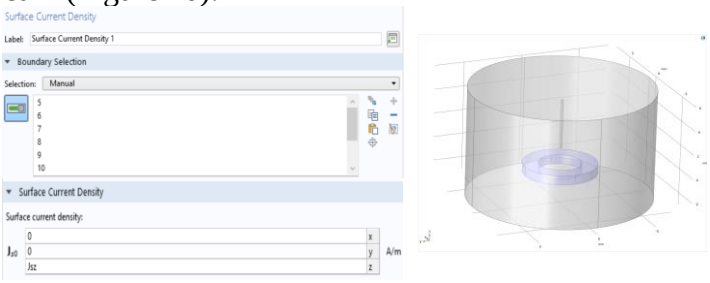

Figure 20. Surface current density

The distribution of the magnetic field was obtained after running the model, based on the first module, Figure 21.

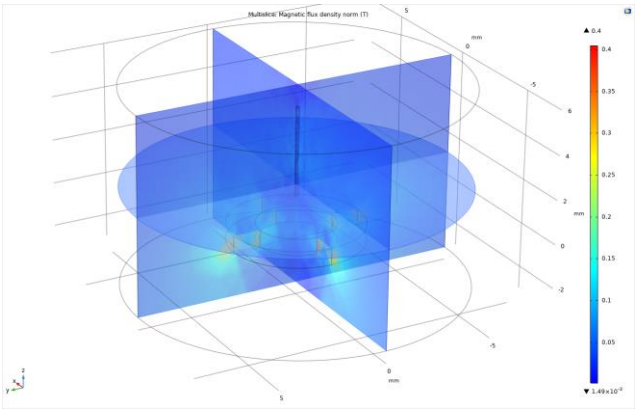

Figure 21. Magnetic flux density for a coil

Charged Particle Tracing study was added aiming at determination of ion beam trajectory within the working space. Thus, the magnetic force was considered, provided by the density flux magnetic module from the previous study (Figure 22).

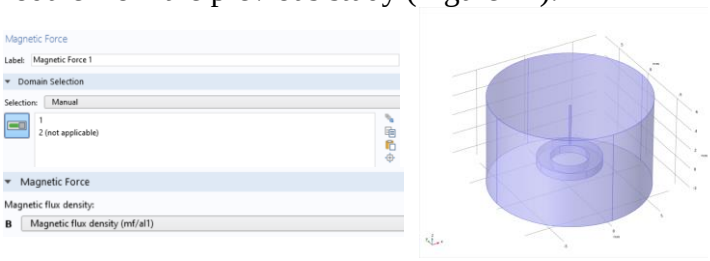

Figure 22. Adding magnetic force

In this case, the particle entry area is defined together with the study settings. So, uniform particle distribution, number of particles released from zone 13 and their initial velocity are in Figure 23.

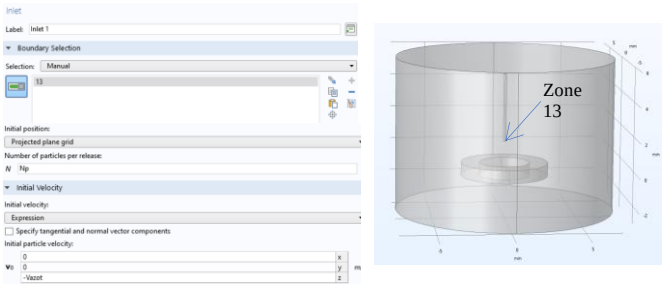

Figure 23. Particle inlet area and beam inlet settings

After running the program, one can see how the ion trajectory remains not deflected, creating conditions for small area deposition on the sample (Figure 24).

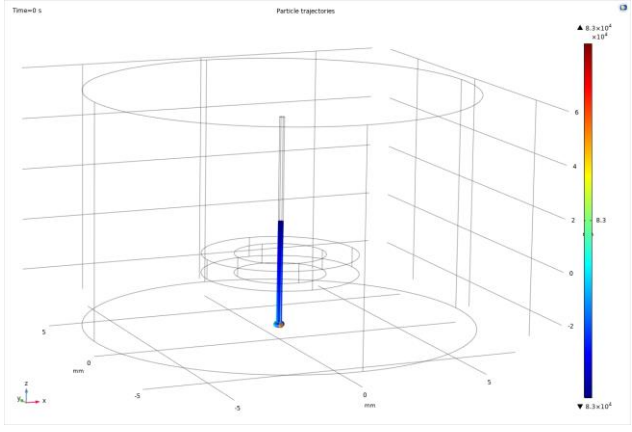

Figure 24. Particle trajectory simulation

Considering the values of the current density on the surface (Jsz), Poincaré maps were visualized to determine the deviation of the ion beam trajectory within the working space. On this purpose, the cut planes used are shown in Figures 25-27.

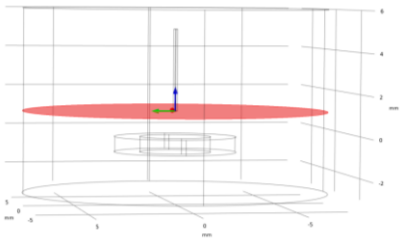

Figure 25. Cut plane 1 with coordinate Z=1

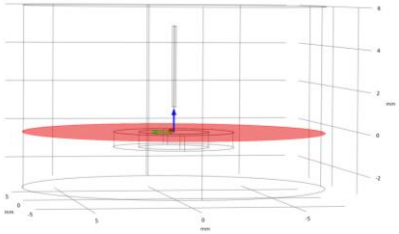

Figure 26. Cut plane 2 with coordinate Z= - 1,25

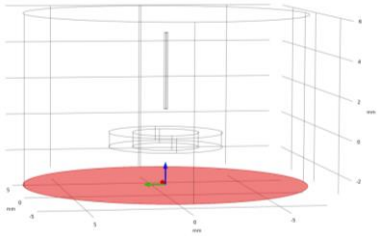

Figure 27. Cut plane 2 with coordinate Z= - 3

6. RESULTS

6.1. The results obtained after the simulation in the COMSOL Multiphysics program for IBM

To study the variations of the output technological parameters, the angle θ was incrementally modified and their graphs are represented in Figures 28-30.

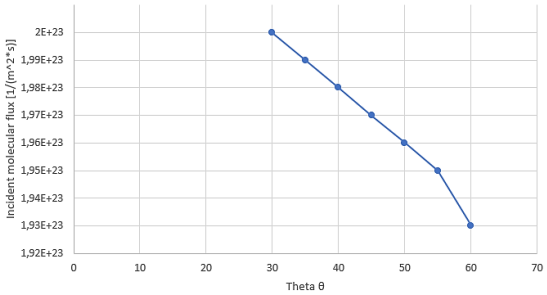

Figure 28. Incident molecular flux variation

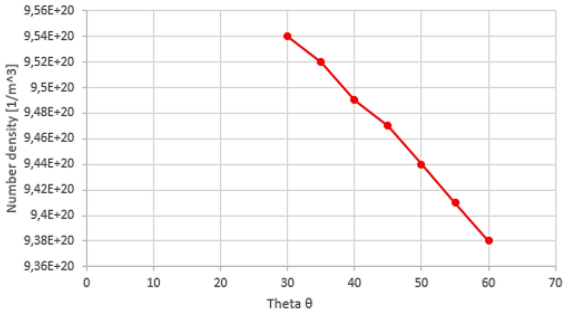

Figure 29. Number density variation

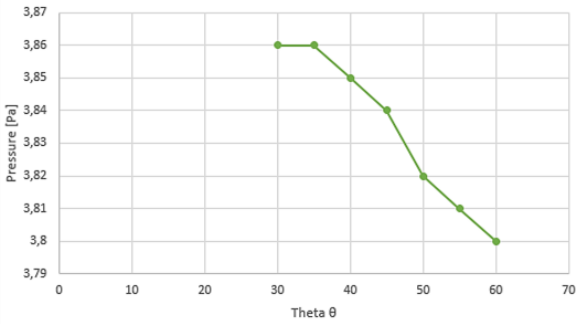

Figure 30. Pressure variation

As one can see, the increase of theta angle of the water relative to incidental direction of ion beam produces a lowering of studied output parameters.

6.2. The results obtained after the simulation in the COMSOL Multiphysics program for EDD

For reaching the values of the magnetic flux from table 1, the Jsz values were modified, and the correspondence between these parameters is presented in table 2, resulted from study 1 running.

Table 2. Jsz values related to magnetic flux

Parameters	Levels				
Magnetic flux, Tesla	0.04	0.07	0.16	0.20	0.40
Surface current density (Jzs), A/m	60000	90000	220000	270000	550000

If the current density increases, it is observed that there is a deviation of the ion trajectory on the target surface as Poincaré graphs indicated in Figures 31-35, in relation to Jsz values. Each previous cut plane has a corresponding color, respectively: Z=1, red; Z= -1,25, black; Z= -3, blue.

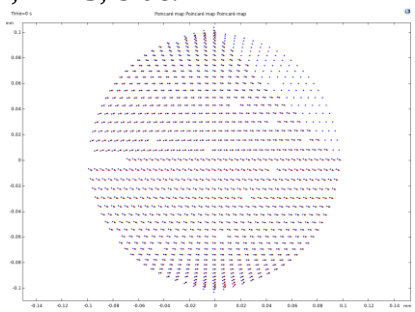

Figure 31. Poincaré map for Jsz = 60000

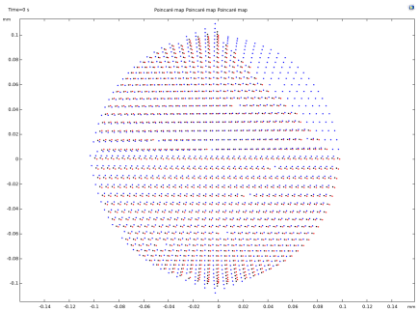

Figure 32. Poincaré map for Jsz = 90000

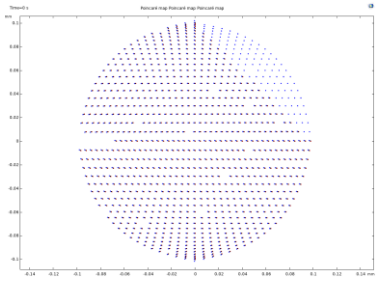

Figure 33. Poincaré map for Jsz = 22000

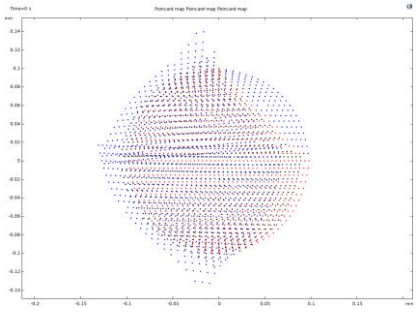

Figure 34. Poincaré map for Jsz = 27000

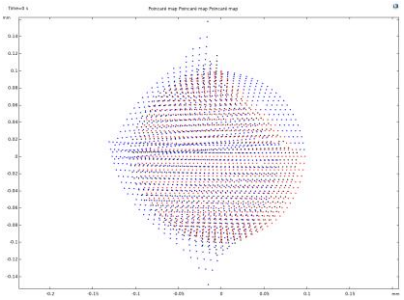

Figure 35. Poincaré map for Jsz = 55000

7. CONCLUSION

Based on this numerical simulation of ion implantation, it can be concluded: if wafer theta angle increases in the interval 30-60^o, the molecular flux, the number density variation, and the numerical density decrease. The position of the sample theta value of 30^o relative to incidental direction of ions beam improves the studied output parameters.

The numerical simulation of EDD process indicated that the distribution of particles on Al alloy sample could be kept under control by ED parameters of discharge and magnetic flux. The material deposition dimensions are framed into 0.2 – 0.3 mm spot if the tool has similar diameter. If the surface current density is increase, a larger and more irregulate distribution on the sample resulted with an optimum distribution at a mean value of magnetic flux.

Further experimental research is needed for validation of numerical simulation of ion implantation and electrical discharge deposition.

8. ACKNOWLEDGEMENT

This work was supported by a grant of the Ministry of Research, Innovation and Digitization, CNCS/CCCDI – UEFISCDI, project number PN-III-P2-2.2-PED-2019-0367, within PNCDI III.

9. REFERENCES

1. Jingyi Yue, Yan Cao, Corrosion Prevention by Applied Coatings on Aluminium Alloy in Corrosive Environments, *International journal of electrochemical science*, June (2015).
2. J. Wood, Gautam Majumdar, Ion Implantation, *Reference Module in Materials Science and Materials Engineering* (2016).
3. Bandriyana, A.H.I. et. al., Microstructure and oxidation behavior of high strength steel AISI 410 implanted with nitrogen ion, *AIP Conference Proceedings* 1725, 020010 (2016).
4. Nurdin, A. et. al., Assessment of fatigue and corrosion fatigue behaviours of the nitrogen ion implanted CpTi, *International Journal of Fatigue 61*, (2014).
5. Chatti, S., Laperriere, L., Reinhart, G., Tolio, T., *CIRP Encyclopedia of Production Engineering*, Springer, (2019).
6. COMSOL Multiphysics - Molecular Flow in an Ion-Implant Vacuum System, available at https://www.comsol.com/model/molecular-flow-in-an-ion-implant-vacuum-system-10011
7. Marinescu, N.I. et al. *Technologies with beams oscillations and jets. Technologies with electron, ion beams and microwaves*, Printech, Bucharest (2018)
8. Kunieda and Kobayshi, Clarifying Mechanism of Determining tool electrode wear ratio in EDM using spectroscopic measurement of vapor density, *Journal of Material Processing Technology*, Vol. 149 (2004)
9. Kunieda, Electric Discharge Machining in a gas, *Annals of CIRP*, vol. 46, January (1997).
10. Lee L., Study of the effect of machining parameters on the machining characteristics in electrical discharge machining of tungsten carbide, *Journal of Material Processing Technology*, vol. 115 (2001).
11. Rahul G. et. al, *Online Monitoring of Electric Discharge Deposition Process*, International Journal Of Computer and Communication Engineering, Vol. 1, No. 2, July (2012)
12. C. M. Abreu et. al., Wear and Corrosion Performance of Two Different Tempers (T6 and T73) of AA7075 Aluminium Alloy After Nitrogen Implantation, *Appl. Surf. Sci.* 327 (2015)
13. Priyantoro, D., Mulyani, E., Sujitno, T., Effect of Hardness, Corrosion Rate, and Crystal Structure of Aluminum, *Advances in Materials.* Vol. 8, No. 4, (2019).
14. Abdi et. al, Surface Nanostructure Modification of Al Substrate Trans. Nonferrous, *Met.*, Soc. China, pg. 701 – 710 (2017).